Mapping the Variability of Soil Texture Based on VIS-NIR Proximal Sensing

Sari Virgawati[1,*], Muhjidin Mawardi[2], Lilik Sutiarso[2],
Sakae Shibusawa[3], Hendrik Segah[4], Masakazu Kodaira[3]

[1]Dept. of Agrotechnology, University of Pembangunan Nasional "Veteran" Yogyakarta, Indonesia
[2]Dept. of Agricultural and Biosystem Engineering, University of Gadjah Mada, Indonesia
[3]Dept. of Environmental and Agric. Engineering, Tokyo University of Agric. and Technology, Japan
[4]Dept. of Forestry, Faculty of Agriculture, University of Palangka Raya, Indonesia
Corresponding author e-mail: sari_virgawati@upnyk.ac.id

Abstract

Soil texture is one of the soil properties influencing most physical, chemical, and biological soil processes. Information on soil texture is important to support the agronomic decisions for farm management. The problem is how to provide reliable, fast and inexpensive information of soil texture in numerous soil samples and repeated measurement. The objective of this research was to generate the soil texture map based on laboratory Vis-NIR (Visible - Near Infra-Red) spectroscopy and inverse distance weighted (IDW) interpolation method. An ASD Fieldspec 3 with a spectral range from 350 nm to 2500 nm was used to measure the soil reflectance. Pipette method was used to measure the silt, clay and sand fractions. The partial least square regression (PLSR) was performed to establish the prediction model of soil texture. The predicted values were mapped and showing the information of spatial and temporal variability of soil texture.

Keywords: Vis-NIR, spectroscopy, soil texture, PLSR, IDW.

1. Introduction

The knowledge of the spatial and temporal variability of soil properties will improve the understanding of the field condition, accordingly, the agricultural actors can make the best decisions with precise treatments for their fields. One of the important properties of soil for agricultural management is the texture of the soil.

Soil texture associated with the ability of soil to retain water, soil moisture content, soil organic matter and minerals which are essential in agriculture. Relative amounts of sand, silt and clay influences porosity, permeability, ease of tillage and nutrient retention. The clay fraction has a significant influence on many physical and chemical processes that occur in soil. In contrast, the sand and silt fraction typically do not have much influence on chemical processes (Jury et al., 2004). Soil texture does not usually change with management practices, however, it may be altered by erosion, deposition, truncation, and some other human interventions (Osman, 2013). Since it has a major effect on the soil fertility levels, information on soil texture is important to support the agronomic decisions for farm management. The problem is how to provide reliable, fast and inexpensive information of soil texture in the subsurface from numerous soil samples and repeated measurement.

Proximal soil sensing techniques have been developed to better understand the soil variability (Adamchuk et al., 2012). It is the use of field-based sensors to obtain signals from the soil when the sensor's detector is in contact with or close to (within 2m) the soil (Viscarra-Rossel et al., 2011). Recently, visible and near-infrared (Vis-NIR) diffuse reflectance spectroscopy has emerged as a rapid and low-cost tool for extensive investigation of soil properties.

Viscarra-Rossel et al. (2016) have developed and analyzed a global soil Vis-NIR spectral library to characterize the world's soil. They recorded the spectra with Fieldspec®, Agrispec®, Terraspec® or Labspec® instruments with a spectral range of 350-2500 nm and mostly with a contact probe® or muglite® lightsource.

There are several soil attributes that often are well estimated with Vis-NIR spectroscopy. The most obvious ones are soil texture, especially clay content, mineralogy, the content of soil organic carbon or soil organic matter and soil water (Stenberg et al., 2010). Soil Vis-NIR reflectance spectra contain valuable information for predicting

soil textural fractions (Conforti et al., 2015). Reflectance was relatively high for soils with loamy sand texture with over 70% sand content.

The quantitative spectral analysis of soil using Vis-NIR reflectance spectroscopy requires sophisticated statistical techniques to discern the response of soil attributes from spectral properties. Various methods have been used to relate a soil spectrum to soil attributes (Gholizadeh et al., 2014).

The most common calibration methods applied are based on linear regressions, namely stepwise multiple linear regression (SMLR), principal component regression (PCR), and partial least squares regression (PLSR). PCR and PLSR techniques can cope with data containing large numbers of predictor variables that are highly collinear. However, PLSR is often preferred by analysts because it relates the response and predictor variables so that the model explains more of the variance in the response with fewer components, it is more interpretable and the algorithm is computationally faster (Stenberg et al., 2010). Viscarra-Rossel et al. (2006) agreed with Geladi and Kowalski (1986) that PLSR takes advantage of the correlation that exists between the spectra and the soil, thus the resulting spectral vectors are directly related to the soil attribute.

The final construction of a map corresponding to a parcel is performed based on the estimation of the values of a variable at non-sampled points, using a spatial interpolation method (Andreo, 2013). There are several interpolation methods, such as IDW (Inverse Distance Weighted), Kriging, Spline, etc. There is no general method that is suitable for all problems; it depends on the nature of the variable and on the time-scale on which the variable is represented (Prim, 2014).

Mapping on spatial and temporal soil variability has been the part of farm management in precision farming activities (Auernhammer et al., 2015). This research offers an integrated method of proximal soil sensing using Vis-NIR spectroscopy to detect the soil properties and the technology for mapping variability using geospatial analysis. With this method, soil testing for numerous samples and repeated measurements are more effective and efficient to arrange the Site Specific Farm Management (SSFM). The objective of this research was to generate the map of soil texture variability based on laboratory Vis-NIR spectroscopy and inverse distance weighted (IDW) interpolation method.

2. The Methods

The research was conducted in three phases of activities i.e. (1) collecting soil data by sampling and measuring the soil properties, (2) data analysis to determine the prediction model of soil properties, and (3) create the spatial and temporal map of soil variability.

2.1. Research Area

The research was conducted at soybean farms in two locations, i.e. Natah Village, Nglipar District, Gunungkidul Regency (7°51'39.0"S, 110°39'19.4"E) and Jatimulyo Village, Dlingo District,

Bantul Regency (7°55'22.5"S, 110°29'08.7"E) in Yogyakarta Province (Fig. 1).

Fig. 1. Location of the research area:
G-field: Nglipar, Gunungkidul; B-field: Dlingo, Bantul
(Background map source: ESRI et al., 2016)

The elevation of Nglipar ranges from 200 to 210 m asl. While Dlingo elevation ranges from 190 to 200 m asl. The slope varies between 5° to 10° which Dlingo was steeper than Nglipar.

2.2. Materials and Instruments

Soil was the main material to be observed in this research. The instruments used were:
a. Soil sampling tools (auger, trowel, bucket, sticks, zip lock plastic bag, marker, etc.).
b. GPS Garmin 60 csx.
c. Ring samples (*Eijkelkamp*) with 5 cm height and 5 cm diameter.
d. The Analytical Spectral Devices *FieldSpec*® 3 (ASD Inc., Boulder, Colorado, USA), a portable spectroradiometer with a spectral range from 350 nm to 2500 nm.
e. *Spectralon*® Diffuse Reflectance Standard, a white reference panel for reflectance calibration.
f. Black aluminum ring plate to hold up the ASD probe vertically (modified by TUAT Laboratory),
g. A set of tools for texture analysis in soil Lab.

2.3. Soil Sampling

Due to the irregular and terrace shapes of the fields (Fig. 2), the layout of sample points was set up using the grid method combined with a transect line of a 5-meter interval. In Google Earth the terrain data is available and the users can create their own points and areas of interest (Lubis et al., 2017). There were 30 sample points for each field marked with bamboo sticks. The coordinates of the field boundaries and sampling points were recorded using GPS. The soil was sampled at 2 stages within one cropping season from October 2016 to January 2017, i.e. before planting and after harvesting the soybeans. Each point was taken using auger at a depth of 5-15 cm. The total samples from 2 locations and 2 stages sampling were 40 samples for texture analysis and 120 samples for spectroscopic measurements. All samples were air-

dried, then gently crushed to break up larger aggregates, afterwards removed the visible roots and each sample was sieved at 2 mm strainer.
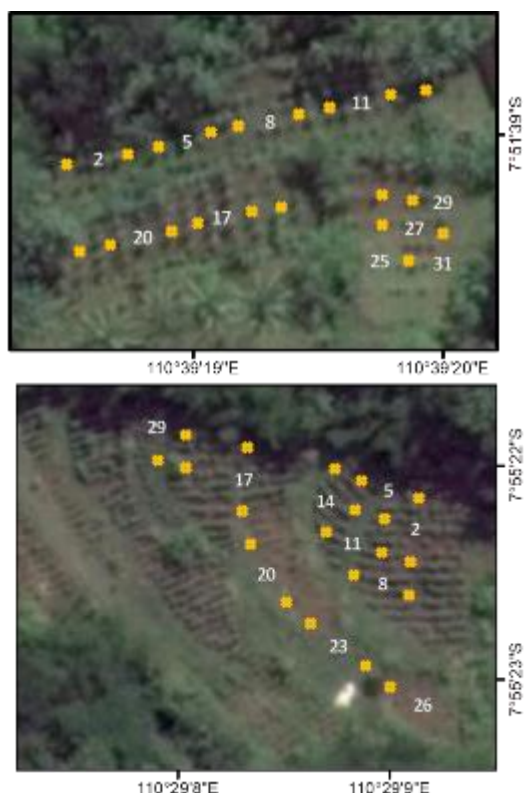
Fig. 2. Sampling layout. *above*: Nglipar (G) (1500 m2); *below*: Dlingo (B) site (1300 m2)
(Modified from Google Earth 2012)

2.4. Soil texture analysis

The soil texture was analyzed by the Soil Analytical Services Laboratory at UPN "Veteran" Yogyakarta using Robinson's pipette method to determine the percentage of sand, silt, and clay.

2.5. Laboratory Vis-NIR Spectroscopy

The spectroscopy measurement was performed at the Agricultural Laboratory, University of Palangka Raya, Central Kalimantan, using ASD Field-spec® 3 350-2500 nm spectroradiometer. Each soil sample was placed into a 5 cm dia. ring sample (*Eijkelkamp*), and flattened the surface. A black aluminum ring plate (modified by TUAT Laboratory, Japan) was fitted on the top of ring sample in order to hold the ASD probe of the optic sensors and keep the same distance from the probe tip to the sample surface (Fig. 3).

Fig. 3. Soil reflectance measurement.
left: soils in ring sample
right: The ASD probe was inserted into a black aluminum ring plate at the sample surface

The reflectance of each sample was scanned 10 times with different positions by moving the ring sample circularly, and the results averaged in post-processing. Every 15 minutes the instrument was calibrated to a reflectance standard by scanning the white *spectralon* panel. The reflectance value of each spectrum was recorded in the computer accompanied by the instrument. A ViewSpecPro software had been installed to translate from binary to ASCII.

2.6. Multivariate Statistical Analysis

The data of soil texture was compiled in a worksheet of MS Excel with such format compatible to be exported to the Unscrambler X software to perform the multivariate analysis. The measured reflectance (R) spectra were transformed in absorbance through the log (1/R) to reduce noise, offset effects, and to enhance the linearity between the measured absorbance and soil properties (Conforti et al., 2015). To enhance weak signals and remove noise due to diffuse reflection, the absorbance spectra were pre-treated using the second derivative Savitzky and Golay method (Gholozadeh et al., 2014). Moreover, both edges of the spectra were removed as these parts of the spectra were unstable and rich in noise (Aliyah et al., 2015).

The calibration models were subsequently developed by applying the partial least-square regression (PLSR) technique coupled with full cross-validation to establish the relationship between the referenced value of soil textures with the pre-treated Vis-NIR soil absorbance spectra from the corresponding locations (Aliyah et al., 2015). Three calibration models were developed, i.e. sand, silt and clay models for each location.

The selection criteria of any pretreatments were the largest coefficient of multiple determinations (R^2) and the smallest of Root Mean Square Error (RMSE). The full cross-validation ability of PLSR was given by the value of residual prediction deviation (RPD). The ability of Vis-NIR to predict values of soil properties can be grouped into three categories based on RPD values: category **A** or excellent (RPD >2.0) includes soil properties with measured vs. predicted R^2 values between 0.80 and 1.00; category **B** or good (RPD = 1.4~2.0) and R^2 values between 0.50 and 0.80, and category **C** or unreliable (RPD <1.4;) and R^2 < 0.50 (Chang et al., 2001). RPD was given by the ratio of the standard deviation (SD) of the reference dataset to the root mean square error of full cross-validation ($RMSE_{val}$), as in Equation (1):

$$RPD = SD. RMSE_{val}^{-1} \qquad (1)$$

The selected calibration model was used to predict the soil textural fraction of new samples.

2.7. Mapping the soil texture variability

The ArcGIS v10.2 software was applied to create the map of soil texture variability. The soil

110

texture prediction values of all recorded sample points coordinates were compiled in one excel worksheet and used as a database (*.mxd file) to create feature classes or shapefiles (*.shp file) from the catalog in ArcGIS. The position of sample points in each field were drawn as a basemap layer to all given information in the attribute table. The geostatistical analyst with inverse distance weighting (IDW) method was used to perform the spatial interpolation.

3. Result and Discussion

3.1. Site Description

Nglipar and Dlingo had a tropical climate and classified as Am by Köppen and Geiger. The average annual temperatures of Nglipar and Dlingo were 25.2°C and 25.8°C, and the average rainfalls were 2,083 mm and 2,019 mm (Merkel, 2017).

Soil types in the study area were classified as Hapludults and Dystrudepts at Nglipar, while at Dlingo were classified as Hapludalfs, Eutrudepts, and Udorthents (BBSDLP, 2016).

The texture of all soil samples in this research were classified as *clay.*

3.2. Soil Reflectance

Soil texture affects soil optical properties. Light is trapped in the rough surfaces of the coarse soil particles. For example, if iron and lime are present, a stronger reflectance is received than if the soil material was fine textured and dry.

Variations in soil reflectance occur where there is a change in the distribution of light and shadow areas with surface roughness areas (Sahu, 2008). Fig. 4 presents the soils reflectance of Nglipar (G) and Dlingo (B), measured before planting and after harvesting.
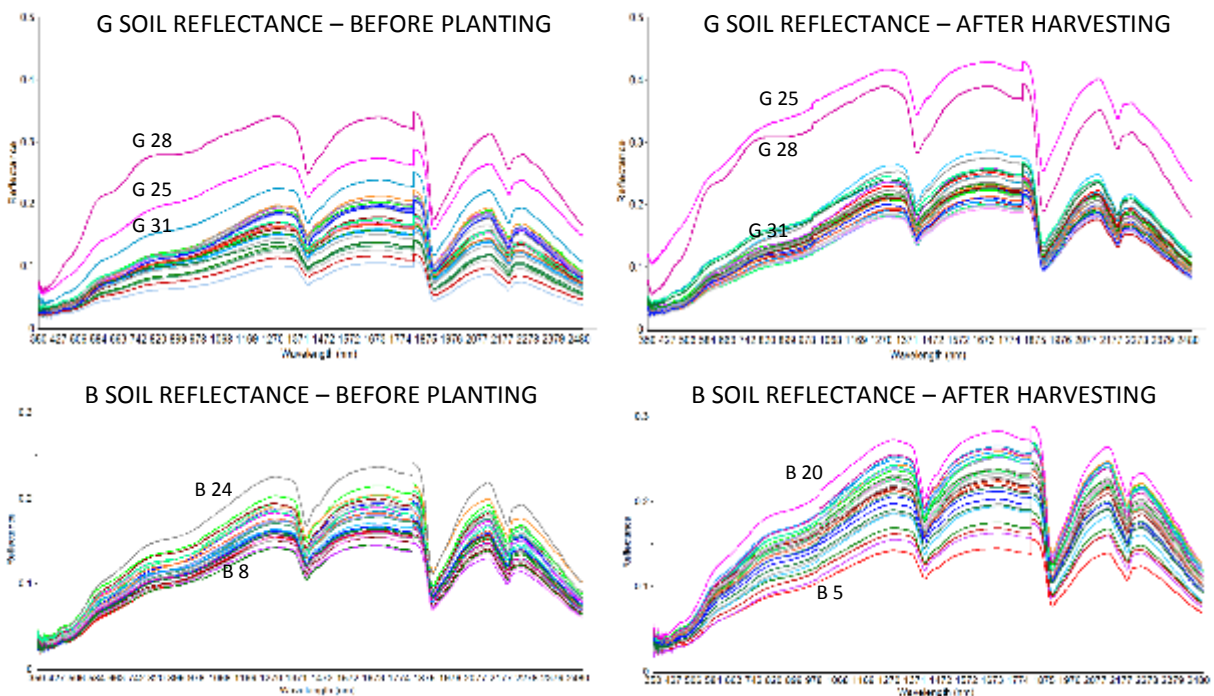
Fig. 4. The soil reflece of Nglipar (above) and Dlingo (below) before planting and after harvesting

3.3. The Soil Texture Prediction Model

The data used in PLSR were recalculated to find the best calibration model by removing the outliers at maximum 4 samples. The summary of PLSR results is shown in Table 4.

The prediction model that shows the correlation between the soil reflectance and soil property are written in the matrix form as shown in Equation 2. For soil texture prediction models, the matrices are presented in Equations 3, 4 and 5.

The better results obtained by using the PLSR method are clearly due to the fact that PLSR takes advantage of the use of the entire spectral signature (Curcio et al., 2013). The regression coefficient plotted in Fig. 5 shows the investigated spectrum that should be considered important for the prediction of soil textures. The size of the regression

coefficients represents the importance of the absorption band.

Table 4. Summary of PLSR Results and RPD for Textural Fraction Calibration Models

Location	G (Nglipar, GK)			B (Dlingo, Bantul)		
PLSR result	*Sand*	*Silt*	*Clay*	*Sand*	*Silt*	*Clay*
Used samples	16	16	16	16	16	16
R^2_{cal}	0.99	0.99	0.99	0.99	0.99	0.99
$RMSE_{cal}$	0.18	0.16	0.23	0.35	0.28	0.10
R^2_{val}	0.67	0.79	0.83	0.69	0.44	0.41
$RMSE_{val}$	2.95	2.07	2.77	2.67	2.80	2.62
SD	4.72	4.60	6.01	4.40	3.56	3.57
RPD value	1.60	2.22	2.17	1.65	1.27	1.36

111

category*	B	A	A	B	C	C

$$\begin{pmatrix} y_G \\ y_B \end{pmatrix} = \begin{pmatrix} 1 & S_{G600} & S_{G610} & \dots & S_{G2300} \\ 1 & S_{B600} & S_{B610} & \dots & S_{B2300} \end{pmatrix} \begin{pmatrix} \beta_{G0} & \beta_{B0} \\ \beta_{G600} & \beta_{B600} \\ \beta_{G610} & \beta_{B610} \\ \vdots & \vdots \\ \beta_{G2300} & \beta_{B2300} \end{pmatrix} + \begin{pmatrix} \varepsilon_G \\ \varepsilon_B \end{pmatrix} \quad [2]$$

where:

y   are the soil property value

S   are the 2nd derivative absorption spectra value

600, 610,..., 2300
  are the selected wavelength from 600 nm to 2300 nm with 10 nm interval

β   are the regression coefficients

ε   are the random error

G, B stand for research location G (Gunungkidul) and B (Bantul)

Sand Fraction Prediction Model

$$\begin{pmatrix} Sand_G \\ Sand_B \end{pmatrix} = \begin{pmatrix} 1 & S_{G600} & S_{G610} & \dots & S_{G2300} \\ 1 & S_{B600} & S_{B610} & \dots & S_{B2300} \end{pmatrix} \begin{pmatrix} 32.71 & 28.23 \\ -20001.4 & -13738.2 \\ 3507.4 & -5018.4 \\ \vdots & \vdots \\ -6728.7 & -23726.4 \end{pmatrix} + \begin{pmatrix} \varepsilon_G \\ \varepsilon_B \end{pmatrix} [3]$$

Silt Fraction Prediction Model

$$\begin{pmatrix} Silt_G \\ Silt_B \end{pmatrix} = \begin{pmatrix} 1 & S_{G600} & S_{G610} & \dots & S_{G2300} \\ 1 & S_{B600} & S_{B610} & \dots & S_{B2300} \end{pmatrix} \begin{pmatrix} 13.91 & 38.37 \\ 3996.3 & 2497.3 \\ 6348.3 & -8953.6 \\ \vdots & \vdots \\ 1617.0 & 8273.7 \end{pmatrix} + \begin{pmatrix} \varepsilon_G \\ \varepsilon_B \end{pmatrix} \quad [4]$$

Clay Fraction Prediction Model

$$\begin{pmatrix} Clay_G \\ CLay_B \end{pmatrix} = \begin{pmatrix} 1 & S_{G600} & S_{G610} & \dots & S_{G2300} \\ 1 & S_{B600} & S_{B610} & \dots & S_{B2300} \end{pmatrix} \begin{pmatrix} 55.39 & 46.67 \\ 15878.9 & 12431.8 \\ -24354.3 & 6223.1 \\ \vdots & \vdots \\ 12857.3 & -4972.0 \end{pmatrix} + \begin{pmatrix} \varepsilon_G \\ \varepsilon_B \end{pmatrix} \quad [5]$$
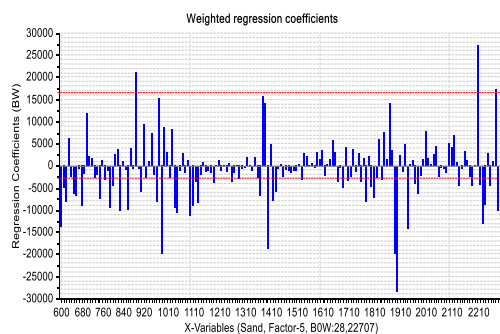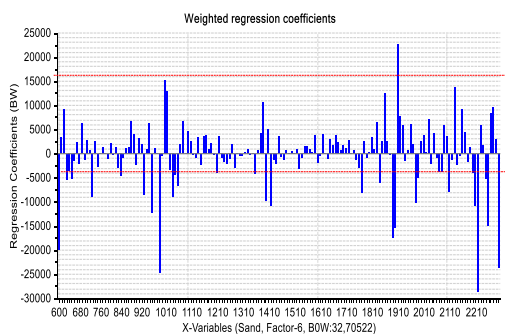
Fig. 5a. The regression coefficients of Sand-G (left) and Sand-B (right)
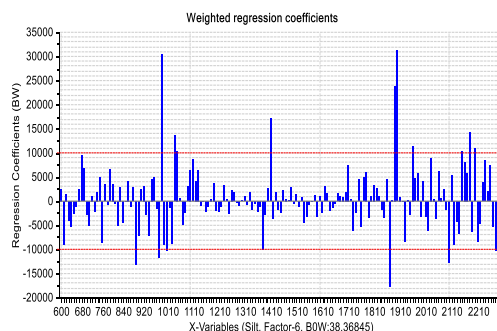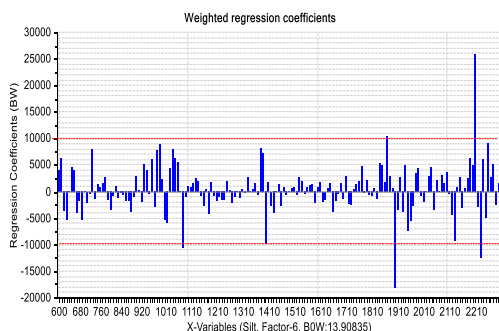
Fig. 5b. The regression coefficients of Silt-G (left) and Silt-B (right)
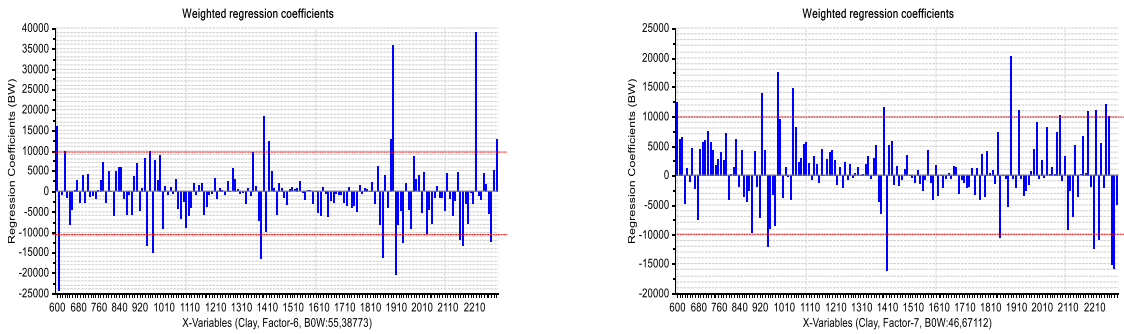
Figure 5c. The regression coefficients of Clay-G (left) and Clay-B (right)

3.4. The Spatial and Temporal Variability Map

The results of mapping using IDW interpolation method are presented in Fig. 8 for Nglipar (G) soils and Fig. 6 for Dlingo (B). In these spatial and temporal variability maps, the predicted soil fractional contents were grouped by 5% interval value with the gradual color base.

Though all the soil samples were classified as clay texture, the fractional distribution had shifted during the growth stages. This movement probably caused by many factors, such as the terraced shape that made soil deposition through run-off.
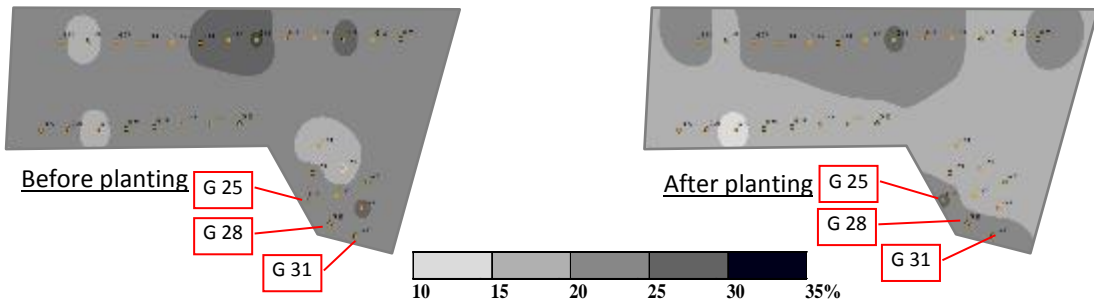
Fig. 6a. The spatial and temporal maps of sand variability at Nglipar (G)
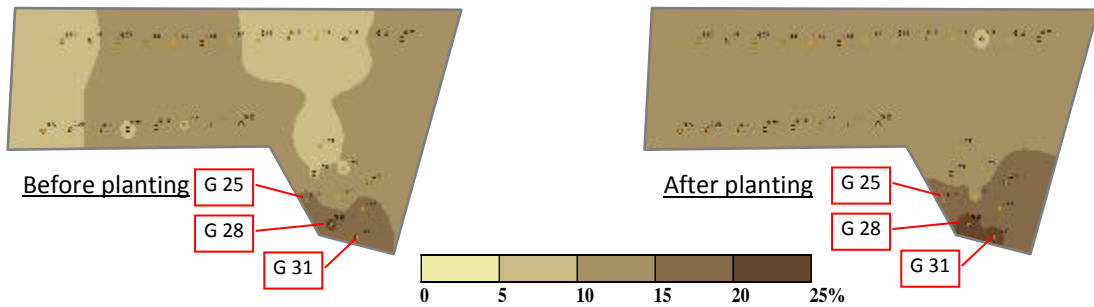
Fig. 6b. The spatial and temporal maps of silt variability at Nglipar (G)
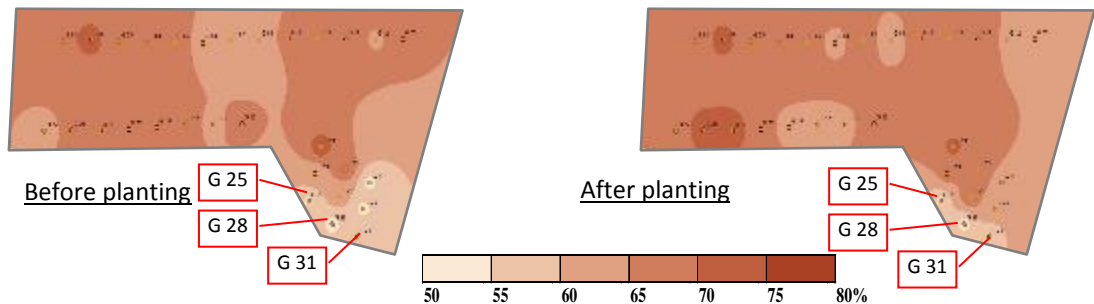
Fig. 6c. The spatial and temporal maps of clay variability at Nglipar (G)
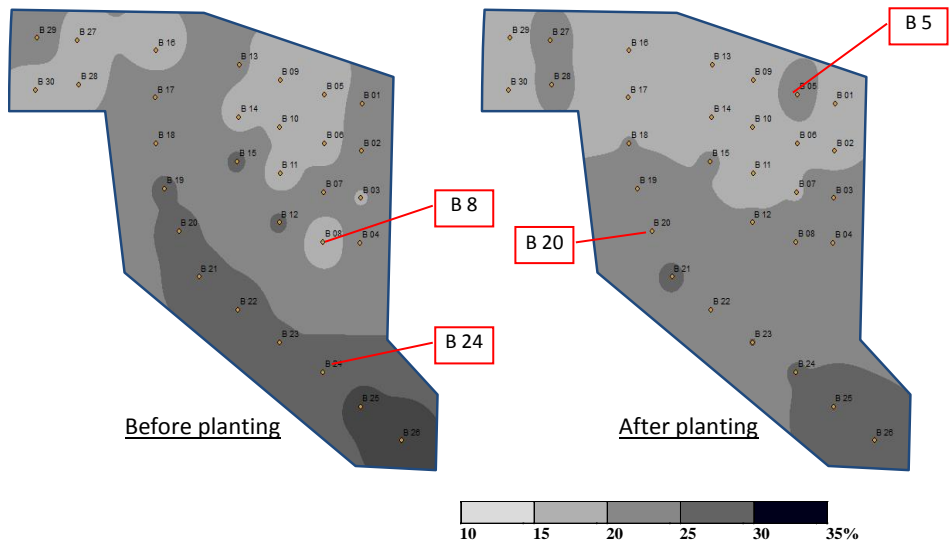
Fig. 6d. The spatial and temporal maps of sand variability at Dlingo (B)
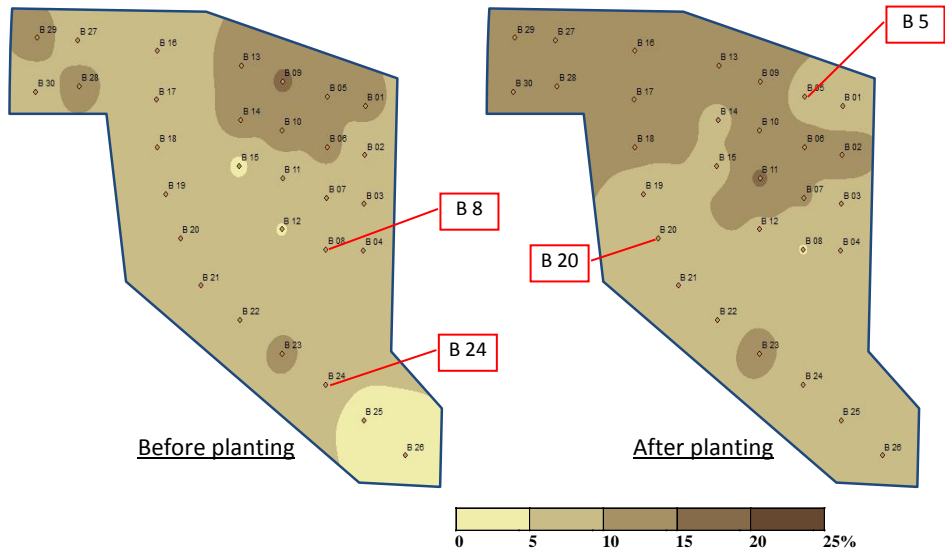
Fig. 6e. The spatial and temporal maps of silt variability at Dlingo (B)
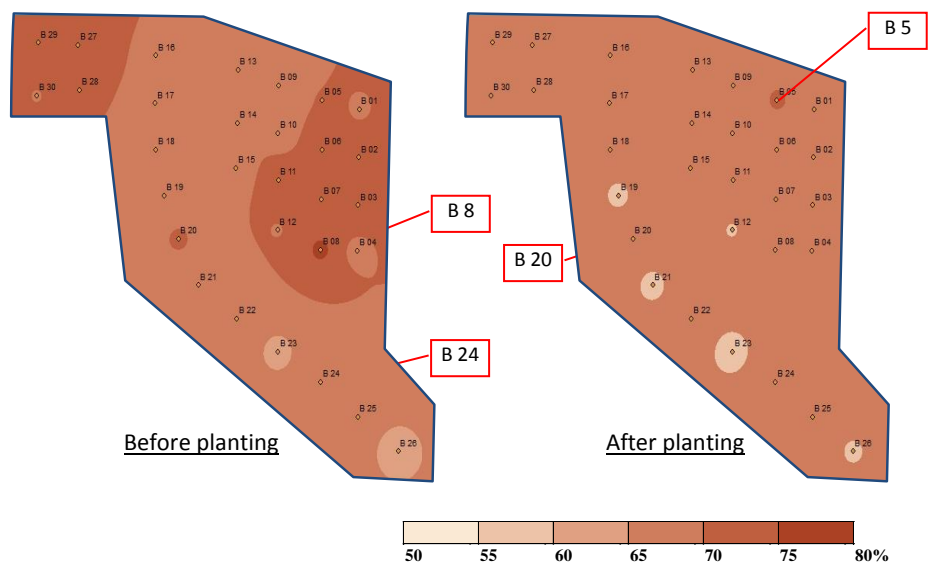
Fig. 6f. The spatial and temporal map of clay variability at Dlingo (B)

114

From the reflectance graph of Nglipar (G) and Dlingo (B) soils in Fig. 6, the samples of G25, G28, G31, B05, B08, B20, and B24 were taken as examples to interpret the relationship between the prediction value described in Fig. 8 and 9. The lower clay content of Nglipar (G) soil showed higher reflectance, and vice versa, the higher clay content of Dlingo (B) soil performed lower reflectance. It seemed the mixture of more sand, more silt, and less clay would result in higher reflectance for Nglipar (G) soil, but it did not work for Dlingo (B) soil. This trends also could be explained statistically by the R^2_{val} and RPD values (Table 4). The model of Nglipar (G) soil able to predict silt and clay content with excellent performance ($R^2_{val} \geq 0.8$; RPD > 2), while the model of Dlingo (B) soil were unreliable to predict silt and clay ($R^2_{val} < 0.5$; RPD < 1.4).

The selection of the spectral data pretreatment process, such as the derivative order, the number of smoothing point, and removing some parts of the spectra, was following a trial and error procedure. It needs to make more trial to find the best pretreatment and Vis–NIR wavelength ranges. The selection of interpolation method also affects the information in the map that may be inconsistent with the predicted appearance in the field. Furthermore, in this study, the elevation difference between the sample points was not taken into account, whereas this would greatly affect the value of predicted soil properties in the terraced field.

4. Conclusion

The ability of Vis-NIR spectra to predict the soil fractional content using PLSR method resulted in different performance. Referring to the model accuracy classification using RPD value, the selected calibration models proved a *good* performance of sand prediction for Nglipar and Dlingo soils. The prediction of silt and clay showed *excellent* performance for Nglipar, while for Dlingo the selected model showed *unreliable* performance to predict its silt and clay. Different pretreatment process of spectral data should be performed in order to improve the correlations between the measured soil fractional content and the spectra. The elevation of each sample point in the terrace field should be included in the calculation so that the predicted value of the interpolation result can be more accurate. For the best result, another interpolation method needs to be compared in order to obtain more accurate results. This research was not only conducting the soil texture mapping but also mapping other soil properties, i.e. soil moisture, pH, soil organic matter, N, P, K, Fe, and CEC, using the same method. Hopefully, this conceptual framework of using the Vis-NIR spectroscopy could be developed to accelerate the mapping of soil variability in Indonesia.

References

Adamchuk, V.I., Allred, B.A., & Viscarra- Rossel, R.A. (2012). Proximal Soil Sensing: Global Perspective. *FastTime, 17* (1). Retrieved from http://www.eegs.org.

Baharom, S. N. A., Shibusawa, S., Kodaira, M., & Kanda, R. (2015). Multiple-depth mapping of soil properties using a visible and near infrared real-time soil sensor for a paddy field. Engineering in Agriculture, Environment and Food, 8(1), 13-17.

Andreo, V. (2013). Remote Sensing and Geographic Information Systems in Precision Farming. Retrieved from http://aulavirtual.ig. conae.gov.ar/ moodle/pluginfile.php/513/ mod_ page/content/ 71/seminario_andreo_2013.pdf.

Auernhammer, H., & Demmel, M. (2015). State of the Art and Future Requirements. In Qin Zhang (Ed.): *Precision Agriculture Technology for Crop Farming*. CRC Press. USA. ISBN: 978-1-4822-5108-1.

BBSDLP. (2016). Datasheet and map files of Nglipar and Dlingo. *Soil Map Scale 1:250,000*. Balai Besar Sumber Daya Lahan Pertanian, Bogor (via email: 12.13.16).

Broome, S.W. (2016). *Soil Physical Properties* [Lecture notes]. Retrieved from http://broome. soil.ncsu.edu/ssc012/Lecture/topic8.htm.

Chang, C. W., Laird, D. A., Mausbach, M. J., & Hurburgh, C. R. (2001). Near-infrared reflectance spectroscopy–principal components regression analyses of soil properties. Soil Science Society of America Journal, 65(2), 480-490.

Conforti, M., Froio, R., Matteucci, G., & Buttafuoco, G. (2015). Visible and near infrared spectroscopy for predicting texture in forest soil: an application in southern Italy. iForest-Biogeosciences and Forestry, 8(3), 339.

Curcio, D., Ciraolo, G., D'Asaro, F., & Minacapilli, M. (2013). Prediction of soil texture distributions using VNIR-SWIR reflectance spectroscopy. Procedia Environmental Sciences, 19, 494-503.

Geladi P. & Kowalski, B.R. (1986). Partial Least-squares Regression: A Tutorial. *Analytica Chimica Acta, 185,* 1-17. https://doi.org/ 10.1016/0003-2670(86)80028-9.

Gholizadeh, A., Amin, M.S.M., Boruvka, L. & Saberioon, M.M. (2014). Models for Paddy Soil Physical Properties Estimation Using Visible and Near Infrared Reflectance Spectroscopy. *Journal of Applied Spectroscopy, 81*(3), 534-540. DOI: 10.1007/s10812-014-9966-x.

Jury, W.A. & Horton, R. (2004). *Soil Physics.* 6th ed. New Jersey, USA: John Wiley & Sons, Inc.

Lubis, M. Z., Anurogo, W., Gustin, O., Hanafi, A., Timbang, D., Rizki, F., ... & Taki, H. M. (2017). Interactive modelling of buildings in Google Earth and GIS: A 3D tool for Urban Planning (Tunjuk Island, Indonesia). Journal of Applied Geospatial Information, 1(2), 44-48.

Merkel, A. (2017). *Climate Data for Cities Worldwide.* Retrieved from http://en.climate-data.org/.

Osman, K.T. (2013). *Soils: Principles, Properties and Management.* Dordrecht, The Netherland: Springer Science+Business Media. https://doi.org/ 10.1111/sum.12053.

Prim, Ashok. (2014). Choosing the Right Interpolation Method. *GIS Resources: A Knowledge Archive.* Retrieved from http://www.gisresources.com/choosing-the-right-interpolation-method_2/.

Sahu, K.C. (2008). *Textbook of Remote Sensing and Geographical Information Systems.* India: Atlantic Publisher.

Stenberg, B., Viscarra-Rossel, R.A., Mouazen, A.M., & Wetterlind, J. (2010). Visible and Near Infrared Spectroscopy in Soil Science. *Advances in Agronomy, 107*, 163-215. http://dx.doi.org/10.1016/S0065-2113(10) 07005-7

Viscarra-Rossel, R.A., Walvoort, D.J.J., McBratney, A.B., Janik, L.J., & Skjemstad, J.O. (2006). Visible, Near Infrared, Mid Infrared or Combined Diffuse Reflectance Spectroscopy for Simultaneous Assessment of Various Soil Properties. *Geoderma, 131* (1-2), 59-75. https://doi.org/10.1016/j.geoderma. 2005. 03.007

Viscarra-Rossel, R.A., Adamchuk, V.I., Sudduth, K.A., McKenzie, N.J., & Lobsey, C. (2011). Proximal Soil Sensing: An Effective Approach for Soil Measurements in Space and Time. *Advances in Agronomy, 113,* 237-282. doi:10.1016/B978-0-12-386473-4.00010-5

Viscarra-Rossel, R.A., Behrens, T., Ben-Dor, E., Brown, D.J., Demattê, J.A.M., Shepherd, K.D., ... Ji, W. (2016). A Global Spectral Library to Characterize the World's Soil. *Earth-Sci. Rev., 155.* http://dx.doi.org/10.1016/j.earscirev.2016. 01.012.